acetylcholinesterase is ruled out by the absence of anticholinesterase activity in the peptide, as indicated in the table.
The observed giant MEPPs were about twice the amplitude of the regular MEPPs and suggest that the contents of 2 regular MEPPs were discharged at the same time, either by the fusion of 2 synaptic vesicles prior to the release[5] or by a 'drag' effect where the release of one vesicle leads to the immediate discharge of another[6].
These results suggest that α-L-aspartyl-L-alanine may have a physiological role in synaptic transmission. The high concentration needed and the long-lasting effect of the dipeptide may imply that it is a relatively weak modulator of cholinergic transmission with a slow but persistent action. It is interesting to note that the dipeptide is a part of the sequence of many naturally occurring peptides, including VIP (vasoactive intestinal peptide), ACTH 18–39, DSIP (delta-sleep-inducing-peptide) and eledoisin.
Basic knowledge of neurotransmission has traditionally accrued mainly from studies on peripheral systems. The usefulness of the phrenic nerve-diaphragm preparation as a prototype for central cholinergic transmission has been repeatedly confirmed. The current experiment demonstrates that this simple system can also be exploited for the study of modulators of the cholinergic system. Since the brain probably contains numerous peptides, many of which have yet to be identified, the inclusion of the nerve-muscle preparation as a first step in the investigation of putative neuromodulators may facilitate the delineation of the functional role of these substances.

Effect of α-L-aspartyl-L-alanine (asp-ala) on cholinesterases

Enzyme tested	Substrate hydrolyzed (nmole/min/incubation tube)
Acetylcholinesterase (4 µg/tube)	6.72 ± 0.34
Acetylcholinesterase (4 µg/tube) + asp-ala (10^{-5} M)	6.82 ± 0.27
Butyrylcholinesterase (2 µg/tube)	7.66 ± 0.26
Butyrylcholinesterase (2 µg/tube) + asp-ala (10^{-5} M)	7.78 ± 0.35

Erythrocyte acetylcholinesterase and serum butyrylcholinesterase (both from Sigma Chemical Co.) were assayed by the dithiobisnitrobenzoate method[4] using acetylthiocholine and butyrylthiocholine as the respective substrates. The enzyme concentrations were chosen so that the products at the endpoint of incubation fell within the linear portion of the dose-response curve. Where indicated asp-ala was added simultaneously with the enzyme. Results are mean of 5 assays ± SD. Statistical analysis shows no significant difference between results in the presence and absence of the peptide.

1 This work was supported by NSF grant BNS 79-00352 and NIH grant CA-27031 to R. Lim.
2 S.T. Cheung and R. Lim, Biochim. biophys. Acta *586*, 418 (1979).
3 D.L. Buchanan, E.E. Haley and R.T. Markiw, Biochemistry *1*, 612 (1962).
4 R. Lim and L.W. Hsu, Biochim. biophys. Acta *249*, 569 (1971).
5 B. Katz, The release of neural transmitter substances. Thomas, Springfield, Il., 1969.
6 A.W. Liley, J. Physiol., Lond. *136*, 595 (1957).

Fourier analysis and spatial representation in the visual cortex

J.J. Kulikowski and P.O. Bishop[1]

Ophthalmic Optics Department, U.M.I.S.T., P.O. Box 88, Manchester M60 1QD (England), and Department of Physiology, John Curtin School of Medical Research, Australian National University, P.O. Box 334, Canberra City, 2601 (Australia),
27 June 1980

Summary. Simple cells in the cat visual cortex are shown to be general purpose analyzers of visual information achieving, at the same time, minimum uncertainty in spatial localization and spatial frequency. Their responses to moving bars, edges and gratings are linearly interrelated and predictable from each other.

Two different approaches to an understanding of the operation of the visual cortex have developed over the past 15 years. One approach, based on the pioneering work of Hubel and Wiesel[2], has concentrated attention on the spatial organization of cortical receptive fields and lines and edges have come to be regarded as the elementary features extracted by simple cells. The alternative approach is based on the application of spatial frequency (Fourier) methods and, by concentrating attention on the sensitivity of cortical neurons to sinusoidal gratings of varying spatial frequencies[3,4], this approach has tended to neglect discrimination of spatial position. It must be stressed however that, for simple cells operating within their linear range, both descriptions are mathematically equivalent: the bar (line) and edge detectors can be represented as cosine and sine components of the Fourier transform[5–7], as was shown earlier by Kulikowski and King-Smith[8] when evaluating line and edge detectors in psychophysical experiments. The present preliminary report aims not only to integrate the 2 approaches mentioned above but also to take into consideration, along lines suggested by Gabor's theory of communications[9,10], the ability of simple cortical cells to localize signals both in spatial position as well as in spatial frequency. Gabor's theory leads to the idea that the visual system attempts to analyze visual information most economically by using pairs of receptive fields of symmetrical (cosine) and antisymmetrical (sine) response profiles, to achieve minimum uncertainty in both spatial localization and spatial frequency. Whereas a symmetrical response profile (figure 1, Ba) has a minimum of 3 subregions (a centrally-located subregion, either ON or OFF, flanked by 2 weaker antagonistic areas), the antisymmetrical profile (figure 1, Ca) has a minimum of 4 subregions (2 approximately equal but antagonistic subregions, one ON the other OFF, located to either side of the centre, each flanked in turn by a very weak antagonistic area[8,11].
If simple cells are amenable to linear analysis[6], the inverse Fourier transform of the spatial frequency tuning curve should predict the spatial response profile. In previous reports[6,7] comparisons have been made between tuning curves prepared with moving gratings and response profiles obtained with stationary flashing stimuli. In our analysis, however, moving stimuli were used in both cases including response profiles to both moving lines (bars) and edges.

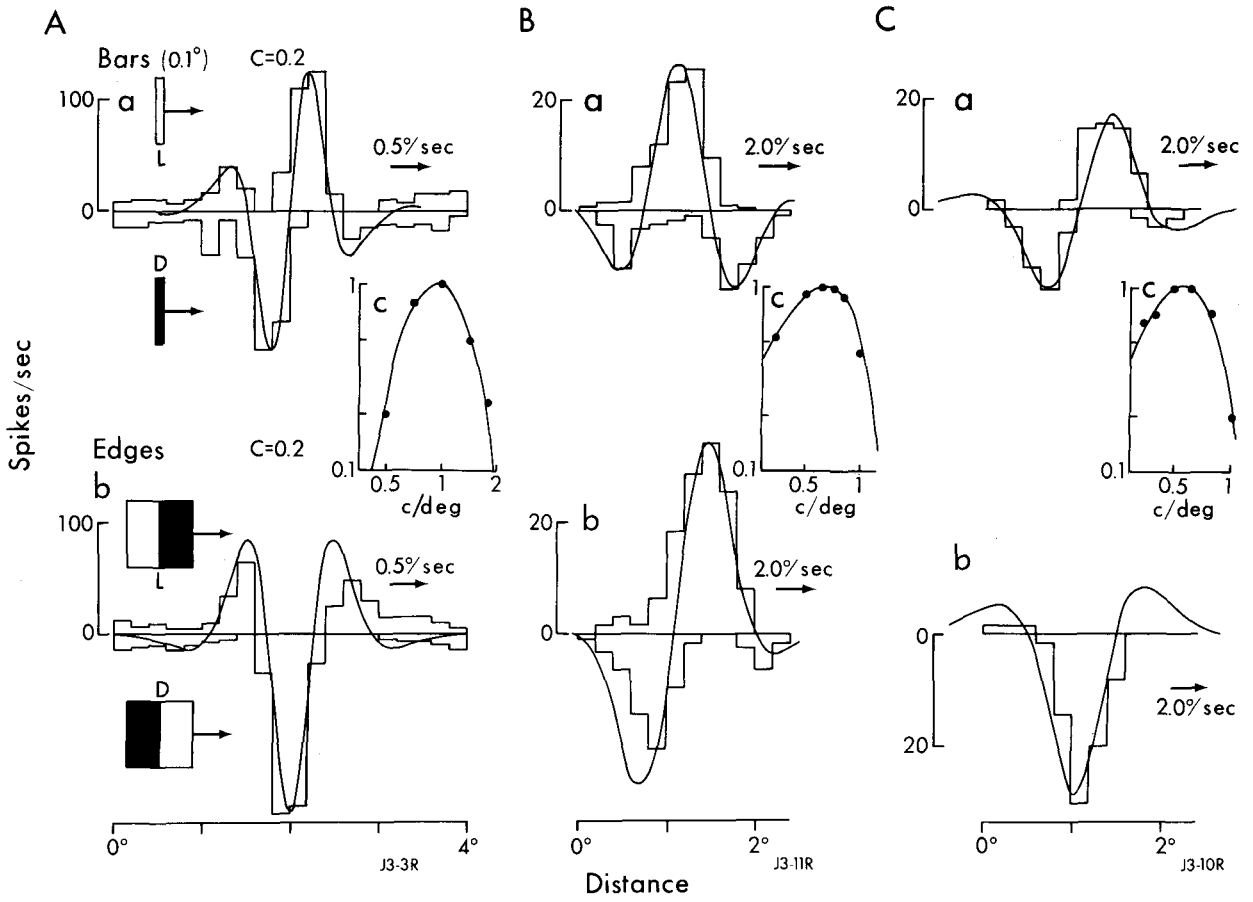

Fig. 1. Average response histograms from 3 simple striate cells (A, Ba and C) to moving bars (a) and edges (b) showing the predictability of these responses from the inverse Fourier transformation (continuous lines) of the respective contrast sensitivity tuning curves (c). The shapes of these tuning curves are chosen to produce the best fit to the data points, thereby testing the predictability of responses to bars and edges (essential for the proper classification of simple cells). However, the fitted tuning curves are not much different from the ideal Gaussian functions for tuning curves with medium and narrow bandwidths ($B_{df} < 1$). Cell A is fitted best by an antisymmetrical profile (sinusoidal Fourier transform), whereas cells B and C are a pair fitted with symmetrical and antisymmetrical profiles respectively.

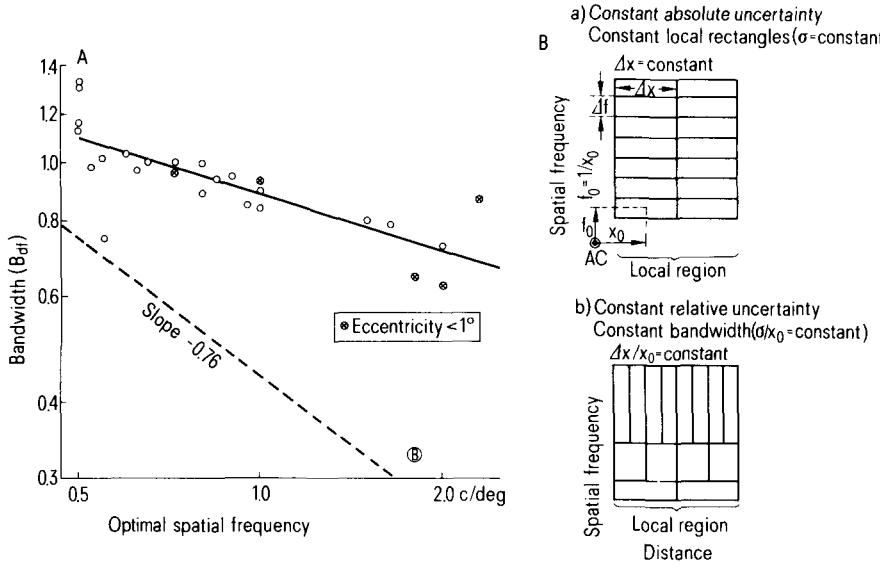

Fig. 2. *A* Bandwidths (B_{df}) of 27 simple cells as a function of optimal spatial frequency, with B_{df} = width of tuning curve (f_u–f_l) at half sensitivity divided by the optimal spatial frequency (f_o). Encircled B marks the relationship for a B cell intermediate in properties between simple and complex cells. *B* Information diagrams symbolizing 2 possible systems in which cortical cells with receptive fields in a given local region of the visual field have either a constant receptive field size (system 'a') or a constant bandwidth (system 'b'). The rectangles in both systems always have the same area, symbolizing the constancy of the product of the uncertainties in spatial position (Δx) and spatial frequencies (Δf), but their shape either remains the same irrespective of f_o (system 'a': constant Δx and Δf) or varies with f_o (system 'b') so that the relative uncertainties ($\Delta x/X_o$ and $\Delta f/f_o$) are constant.

Figure 1 illustrates the recorded response profiles (bar histograms) to moving bars (a) and edges (b) and the predicted response profiles (continuous curves) for 3 simple cells (A, B and C) in the striate cortex of anaesthetized (N_2O/O_2) and paralyzed cats after surgical preparation under halothane. The histograms above and below the baseline are to light and dark bars respectively and similarly for the responses to edges. The predicted curves for moving bars are the inverse Fourier transforms of the respective spatial frequency contrast sensitivity tuning curves to drifting gratings (Ac, Bc and Cc) and the predicted curves for moving edges are integrals of the responses to bars. Cells B and C were selected partly because they lay within 0.1 mm of one another in lamina VI and were remarkably alike in their response properties, with the same preferred stimulus orientation and velocity and having a similar optimal and range of spatial frequencies, but also because the subregions in their receptive fields had symmetrical (B) and antisymmetrical (C) spatial patterns. Not infrequently among our simple cells, the spatial response profiles were not ideally symmetrical and antisymmetrical, the best fit between recorded and predicted profiles being achieved not by the ideal cosine and sine Fourier transforms but by assuming a constant small spatial phase shift from a consinusoidal inverse Fourier transform towards a sinusoidal transform and the reverse. We found good quantitative agreement between predicted and recorded profiles to moving stimuli in about 80% of the simple cells. By contrast only about 50% of the cells showed a reasonable quantitative agreement when the comparison was with spatial profiles to a stationary flashing bar. In our experience the combined use of moving light and dark bars commonly reveals more subregions than are evident with a stationary flashing bar.

Out of 78 cells (11 cats) classified as belonging to the simple family[12], 37 were tested quantitatively with moving bars and edges. Out of the latter group, contrast sensitivity curves to sinusoidal grating drifting at a constant temporal frequency were prepared from 27 by finding the minimum contrast at which a modulated response could no longer be appreciated subjectively[3]. Following Thompson and Tolhurst[13], the bandwidth (B_{df}) of the tuning curves was taken as the full width at half sensitivity (f_u-f_l) divided by the optimal spatial frequency (f_o). The bandwidths ranged from 0.63 to 1.35 (mean, 0.94 or in octaves mean, 1.47). Spatial frequency response curves prepared from 9 of the 27 simple cells showed the bandwidth for responsivity (mean, 0.87) to be slightly narrower than for sensitivity (mean, 1.02) but the difference was not significant. Additionally, quatitative receptive field maps were prepared with stationary flashing bars from 14 cells.

The narrowest bandwidth for the simple family (0.63 or 0.96 octave) was obtained from 2 cells having 5 to 6 subregions, the maximum number we encountered. None of the remaining 10 simple family cells tested with bars and edges, but not gratings, nor any of the 79 simple cells tested quantitatively in an independent study[14], showed more than 4 subregions. The only cells we encountered with a very narrow bandwidth (0.33) belonged to a separate class of neurons (e.g. B in figure 2, A) having properties intermediate between simple and complex with nonlinearity in their responses even to optimal stimulation. To achieve a bandwidth reported to be as narrow as 0.25[13], simple cells with linear and regular receptive fields would need as many as 12 to 13 subregions in their receptive fields. Receptive fields of this kind have yet to be reported.

Gabor's theory[9] implies that full information about visual signals along one axis (x) can be conveyed by pairs of receptive fields having cosine and sine response profiles described by products of a Gaussian envelope and periodic functions.

$$s(x) = e^{-(x-x_0)^2/2\sigma^2} \begin{Bmatrix} \cos \\ \sin \end{Bmatrix} 2\pi f_0 x$$

These functions describe localized harmonic oscillations (antagonistic receptive field subregions) where X_o (figure 2, B) is the distance of the receptive field centre from the visual axis, σ is the SD of the Gaussian envelope of the subregions and f_o is the optimal spatial frequency ($f_o = 1/X_o$, where X_o is the spatial period equal to the width of 2 antagonistic subregions). For these functions, the product of the uncertainties in signalling spatial position (Δx) and spatial frequency (Δf) reaches a theoretical minimum $\Delta x \cdot \Delta f = 1/2$. However the components of the above product may be chosen to reduce one uncertainty at the expense of the other. The information diagrams in figure 2, B symbolize 2 possible extreme systems in which cortical cells with receptive fields in a given local region of the visual field have either a constant receptive field size (system 'a') or a constant bandwidth (system 'b'). The individual rectangles, though representing single cells, are not to be confused with a region (i.e. receptive field) in the visual field. In both systems the rectangles always have the same area, symbolizing the constancy of the product of the uncertainties in spatial position (Δx) and spatial frequency (Δf). If the overall size of the receptive field is constant (constant σ), irrespective of the optimal spatial frequency (f_o), as postulated by Robson[15], both the uncertainties in spatial position and in spatial frequency will be constant, since both depend only on σ, and the rectangles will all be of equal width (Δx) and equal height (Δf). In the alternative system having a constant bandwidth (figure 2, Bb) the relative uncertainties ($\Delta x/X_o$ and $\Delta f/f_o$) are constant. The overall size of the receptive field is now inversely proportional to f_o and hence directly proportional to X_o (σ/X_o = constant). In such a system the number of subregions in the receptive field does not alter with change in receptive field size. The uncertainty in spatial position would decrease in proportion to the reduction in size of the receptive fields, but the uncertainty in spatial frequency would increase as represented by the rectangles of increasing height in figure 2, Bb. Figure 2, A shows that simple cells with higher optimal spatial frequencies (f_o) tend to have tuning curves with narrower bandwidths. Since bandwidth $B_{df} = (f_u - f_l)/f_o$, a regression line with unity slope would mean that the width of the tuning curve (f_u-f_l) would be constant irrespective of the optimal spatial frequency. Furthermore, since the width of the tuning curve (f_u-f_l) is inversely proportional to the SD of the spatial response profile[9], the width of the receptive field would also be independent of the optimal spatial frequency as envisaged in the patch-by-patch model of visual processing proposed by Robson[15]. In this model, linear spatial summation occurs over patches (receptive fields) of constant area despite considerable differences in optimal frequency. Such a model is, however, not supported by the data in figure 2, A where the slope of the regression line is only -0.3 and even the slope of -0.76 indicated by the report of Thompson and Tolhurst[13] falls well short of one.

The decrease in bandwidth with increasing optimal spatial frequency (figure 2, A) appears to rule out the exclusive operation of one or the other of the 2 extreme systems diagrammed in figure 2, B but suggests either that the 2 systems work in parallel over a limited range of spatial frequencies (e.g. 1 octave) or that there is an intermediate type system with a scatter in receptive field sizes and spatial frequency bandwidths. The final picture that emerges from our work is that simple cells are general purpose cells

optimized for processing both spatial position and spatial frequency information and that to regard them as spatial frequency analyzers is stress one side of their function at the expense of the other.

1 We thank Dr S. Marčelja for much helpful discussion.
2 D.H. Hubel and T.N. Wiesel, J. Physiol., Lond. *148,* 574 (1959); J. Physiol., Lond. *160,* 106 (1962).
3 C. Enroth-Cugell and J.G. Robson, J. Physiol., Lond. *187,* 517 (1966).
4 G.F. Cooper and J.G. Robson, in: I.E.E. Conference publ. *42,* 134 (1968).
5 D.G. Tolhurst, in: Spatial Contrast, p.36. Ed. H. Spekreijse and L.H. Van Der Tweel. North-Holland Press, Amsterdam 1977.
6 J.A. Movshon, I.D. Thompson and D.J. Tolhurst, J. Physiol., Lond. *283,* 53 (1978).
7 B.W. Andrews and D.A. Pollen, J. Physiol., Lond. *287,* 163 (1979).
8 J.J. Kulikowski and P.E. King-Smith, Vision Res. *13,* 1455 (1973).
9 D. Gabor, J.I.E.E., Lond. *93,* 429 (1946).
10 S. Marčelja, J. opt. Soc. Am., in press (1981).
11 P.E. King-Smith and J.J. Kulikowski, J. Physiol., Lond. *234,* 5P (1973); J. Physiol., Lond. *247,* 237 (1975).
12 H. Kato, P.O. Bishop and G.A. Orban, J. Neurophysiol. *41,* 1071 (1978).
13 I.D. Thompson and D.J. Tolhurst, J. Physiol., Lond. *295,* 33P (1979).
14 R.M. Camarda, E. Peterhans and P.O. Bishop, in preparation.
15 J.G. Robson, in: Handbook of Perception, vol.5, p.81. Ed. E.C. Carterette and M.P. Friedman. Academic Press, New York 1975.

Effects of later isolation housing on both scent marking behavior and brain cholinergic activites in Mongolian gerbils

H. Yoshimura and K. Manabe[1]

Department of Pharmacology, School of Medicine, Ehime University, Ehime 791-02 (Japan), 2 June 1980

Summary. Significant difference in the frequency of marking was found between aggregated and isolated gerbils. As compared with the aggregated gerbils, isolated gerbils showed high acetylcholinesterase activity in the hippocampus and high choline acetyltransferase activity in the hypothalamus.

The Mongolian gerbil has recently been introduced into physiological and behavioral research. The gerbil marks low-lying objects in the environment by rubbing them with a midventral sebaceous scent gland. Thiessen and his colleagues[2,3] have indicated that the scent marking behavior is closely related to territoriality and dominance status. Brain and Benton[4] have proposed that in mice and rats individual housing alters their territorial dominance. It has also been reported in gerbils that marking behavior was affected by housing conditions[5,6]. In mice and rats, several investigators[7-9] have suggested that the central cholinergic system may play an important role in the mediation of isolation-induced behavioral changes. Little information, however, is available concerning the brain mechanisms of scent marking in the gerbil. This study was conducted to investigate changes in brain cholinergic activities and scent marking behavior in gerbils following later isolation housing.

Materials and methods. Male Mongolian gerbils *(Meriones unguiculatus)* weighing between 60 and 70 g were used. All the animals had free access to food and water. The temperature in the vivarium was maintained at 23 ± 1 °C, and the light-dark cycle (light on at 07.00 h, off at 19.00 h) was kept constant. The open-field apparatus was constructed of gray plexiglass (the size of the floor was 60 × 60 cm, and enclosed by walls 46 cm high), except for a clear side panel which allowed observation from a lateral view. 6 pegs, made from clear plexiglass (2.5 cm long, 1.2 cm wide, and 0.6 cm high), were attached to the floor at regular intervals. Animals were weaned between 23 and 25 days after birth and reared with littermates. At 80 days of age male gerbils were randomly assigned to 2 groups: an isolated (n = 8) and an aggregated group (n = 8, in 2 groups of 4 each). The isolated gerbils were housed in a isolation cage (30 × 19 × 13 cm metal cage), while the aggregated gerbils were housed communally in a 42 × 25 × 15 cm polycarbonate cage (4 ani-

Table 1. Effect of later isolation housing on brain acetylcholinesterase activity in Mongolian gerbils (nmoles acetylthiocholine hydrolyzed/min/mg protein)

Brain areas	Aggregated group (n = 8)	Isolated group (n = 6)
Cortex	40.05 ± 3.18	41.39 ± 2.12
Striatum	534.62 ± 62.84	515.91 ± 61.67
Amygdala	104.51 ± 6.28	109.86 ± 7.72
Hypothalamus	120.26 ± 1.59	121.03 ± 2.88
Midbrain	151.50 ± 5.60	153.66 ± 6.25
Hippocampus	64.77 ± 3.65	69.45 ± 2.99*
Olfactory bulbs	40.75 ± 2.48	41.58 ± 1.54
Pons + medulla oblongata	122.92 ± 4.81	126.19 ± 5.13

Each value is shown as mean ± SD. * Significance was evaluated by means of the 2-tailed Student's t-test comparing the isolated group with the aggregated group ($p < 0.05$).

Table 2. Effect of later isolation housing on brain choline acetyltransferase activity in Mongolian gerbils (nmoles acetylcholine synthesized/h/mg protein)

Brain areas	Aggregated group (n = 8)	Isolated group (n = 6)
Cortex	36.56 ± 2.84	37.20 ± 2.47
Striatum	223.49 ± 21.69	214.60 ± 25.89
Amygdala	99.47 ± 5.59	102.58 ± 8.84
Hypothalamus	53.95 ± 4.02	59.77 ± 4.00*
Midbrain	100.59 ± 4.92	95.91 ± 9.18
Hippocampus	42.13 ± 4.72	43.41 ± 3.68
Olfactory bulbs	24.32 ± 2.21	23.06 ± 1.24
Pons + medulla oblongata	119.20 ± 11.45	123.79 ± 10.51

Each value is shown mean ± SD. * Significance was evaluated by means of the 2-tailed Student's t-test comparing the isolated group with the aggregated group ($p < 0.02$).